

“Quenchbodies”: Quench-Based Antibody Probes That Show Antigen-Dependent Fluorescence

Ryoji Abe,^{†,§} Hiroyuki Ohashi,[‡] Issei Iijima,[†] Masaki Ihara,^{⊥,||} Hiroaki Takagi,[§] Takahiro Hohsaka,[†] and Hiroshi Ueda^{*,‡,⊥}

[†]School of Materials Science, Japan Advanced Institute of Science and Technology, 1-1 Asahidai, Nomi, Ishikawa 923-1292, Japan

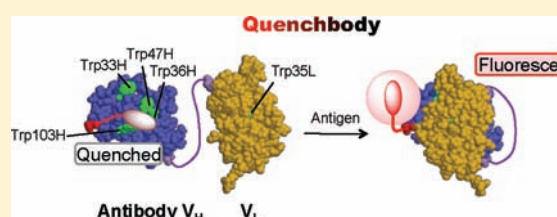
[§]ProteinExpress Company Ltd., 1-8-15 Inohana, Chuo-ku, Chiba 260-0856, Japan

[‡]Department of Chemistry and Biotechnology, School of Engineering, The University of Tokyo, 7-3-Hongo, Bunkyo-ku, Tokyo 113-8656, Japan

[⊥]Department of Bioengineering, School of Engineering, The University of Tokyo, 7-3-1 Hongo, Bunkyo-ku, Tokyo 113-8656, Japan

S Supporting Information

ABSTRACT: Here, we describe a novel reagentless fluorescent biosensor strategy based on the antigen-dependent removal of a quenching effect on a fluorophore attached to antibody domains. Using a cell-free translation-mediated position-specific protein labeling system, we found that an antibody single chain variable region (scFv) that had been fluorolabeled at the N-terminal region showed a significant antigen-dependent fluorescence enhancement. Investigation of the enhancement mechanism by mutagenesis of the carboxytetramethylrhodamine (TAMRA)-labeled anti-osteocalcin scFv showed that antigen-dependency was dependent on semiconserved tryptophan residues near the V_H/V_L interface. This suggested that the binding of the antigen led to the interruption of a quenching effect caused by the proximity of tryptophan residues to the linker-tagged fluorophore. Using TAMRA-scFv, many targets including peptides, proteins, and haptens including morphine-related drugs could be quantified. Similar or higher sensitivities to those observed in competitive ELISA were obtained, even in human plasma. Because of its versatility, this “quenchbody” is expected to have a range of applications, from in vitro diagnostics, to imaging of various targets in situ.



INTRODUCTION

The development of innovative fluorescence-based techniques for probing molecular recognition is of major interest in biophysical chemistry. The naturally occurring amino acid tryptophan (Trp) is of particular interest in fluorescence-based work on peptides and proteins. For example, Trp can serve as an efficient electron donor in photoinduced electron transfer (PET) reactions with certain dye molecules, a property conferred by the Trp indole side chain which is the most readily oxidized functional group among all naturally occurring amino acids.¹

In further promising applications, PET-based biosensors have been developed that use conformationally induced alterations in PET efficiency upon binding for the specific detection of DNA or RNA sequences or antibodies at the single-molecule level.^{2,3} In contrast to Förster resonance energy transfer (FRET)-based systems, in which long-range dipole–dipole interactions are probed, the above sensors require contact formation between the fluorophore and the guanosine or tryptophan residue. Depending on the reduction potential of the fluorophore used, efficient fluorescence quenching via PET can then occur. With careful design of conformationally flexible molecules and the use of appropriate fluorophores, efficient single-molecule sensitive PET sensors can be produced. Therefore, PET-based molecules offer an elegant alternative to conventional biosensors based on FRET processes.

As a possible application for PET-based biosensors, immunological detection of target molecules (immunoassay) is considered as a very attractive area of research. It is an indispensable technique for quantifying various molecules, and is utilized in a range of fields, from basic biological research to clinical diagnostics. Fluorescence-based assays that do not involve separation steps are considered particularly useful, due to advantages such as short assay time and ease of handling. The reagentless fluorescent biosensor approach, which is based on the fluorolabeled antibody fragment whose fluorescence intensity is altered by binding to its target (antigen), is probably the simplest example of such attempts.^{4,5} For example, Bedouelle et al.⁶ and Winter et al.⁷ used site-specifically labeled antibodies that demonstrated increased fluorescence upon binding to their target protein, using the environment-sensitive dye 7-nitrobenz-2-oxa-1,3-diazole (NBD). However, to construct such protein biosensors, the fluorolabeling position on the protein must be optimized, most typically in or near complementarity determining regions (CDR) of the antibody, and this often requires considerable time and labor.

Here, we show a novel strategy of PET-based biosensor for various antigens, using a position-specific protein labeling methodology

Received: July 2, 2011

Published: October 06, 2011

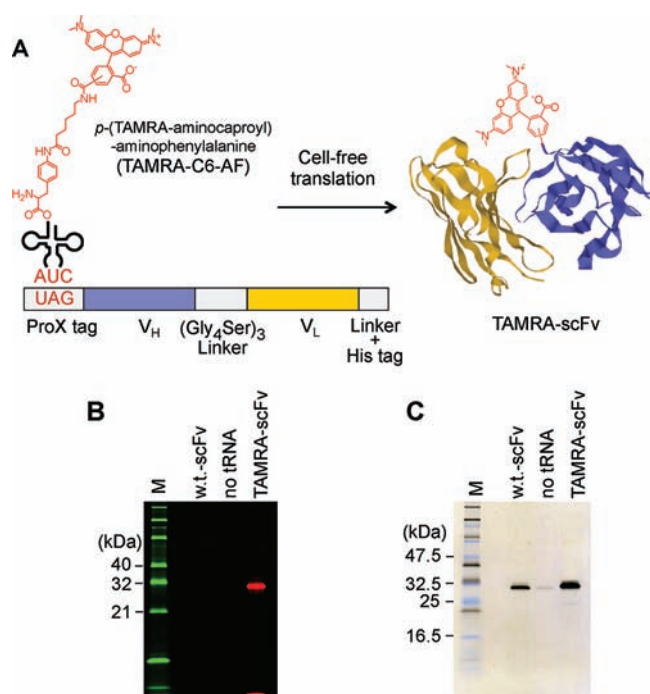


Figure 1. Synthesis of scFv containing TAMRA at the N-terminal region. (A) Illustration of the incorporation of TAMRA-C6-AF into scFv in response to a UAG codon in a cell-free translation system. (B) Fluorescence image of SDS–PAGE for the expression of anti-BGP scFv containing TAMRA-C6-AF. Fluorescence of TAMRA shown in red was detected with excitation at 532 nm and emission at 580 nm. Fluorescent marker shown in green was detected with excitation at 488 nm and emission at 520 nm. (C) Western blot analysis using an anti-His-tag antibody.

based on fluorolabeled aminoacyl tRNA and a cell-free translation system.⁸ During the attempts to make FRET-based biosensor by this methodology, we fortuitously discovered an antigen-dependent fluorescence enhancement of a single chain variable region fragment (scFv) of the antibody fluorolabeled at its N-terminal region. After investigation of the mechanism, it was found that this enhancement was observed due to the quenching of used dye by the semiconserved Trp residues in scFv, probably by PET mechanism. According to the proposed mechanism, the phenomenon was considered to have generality to other antibodies, and it was experimentally confirmed to be indeed the case.

RESULTS

Position-Specific Incorporation of TAMRA-Labeled Amino Acid into Anti-BGP scFv. As the model antibody to apply position-specific fluorolabeling technology, we chose anti-human osteocalcin (bone gla protein, BGP) scFv as the recognition unit for the bone-related disease marker, and as the model dye we took 5-carboxytetramethylrhodamine (TAMRA). This combination was chosen because the variable region, Fv, of this antibody has an interesting property that it is markedly stabilized by bound BGP or its C-terminal epitope peptides.⁹ Also, we have found in other experiments (Abe et al., in preparation) that position-specifically TAMRA-labeled anti-BGP Fv at the N-terminal region of heavy chain variable region V_H demonstrates a modest but significant (1.7-fold) antigen-dependent fluorescence intensity change. To prepare this construct, the two

variable region genes (V_H and V_L) of the anti-BGP antibody obtained from murine hybridoma KTM-219 cells were linked via a gene encoding a (Gly₄Ser)₃ linker (Figure 1A). The incorporation of *p*-(TAMRA-aminocaproyl)-aminophenylalanine (TAMRA-C6-AF) into the N-terminus of the scFv was carried out using the amber suppression method with an N-terminal ProX tag sequence (NH₂-MSKQIEVNXSNE-COOH). This tag is an optimized 12 amino acid sequence containing an amber codon (X) at the ninth position to enhance the incorporation of non-natural amino acids as well as protein expression.¹⁰ In addition, a His tag was fused at the C-terminus of scFv to allow ready detection and purification. The amber codon was decoded by a highly efficient amber suppressor tRNA derived from *Mycoplasma capricolum* Trp₁ tRNA,¹¹ which had been amino-acylated with TAMRA-C6-AF. The TAMRA-C6-AF-tRNA was added to an *Escherichia coli* cell-free translation system, together with the scFv genes fused with a ProX coding sequence. The translation products were resolved by SDS–PAGE and detected by fluorescence imaging of the gel. A clear fluorescent band showing TAMRA fluorescence was observed at the expected molecular weight (32 kDa) (Figure 1B). This result indicated that scFv containing TAMRA at the N-terminal region had been successfully expressed. The scFv was also analyzed by Western blotting using an anti-His tag antibody. The full-length protein was clearly observed in the presence of TAMRA-C6-AF-tRNA, while a negligible amount of the protein was observed in the absence of the suppressor tRNA (Figure 1C). These results indicated that the TAMRA-C6-AF-tRNA decoded the amber codon specifically, and that anti-BGP scFv had been site-specifically and near-quantitatively labeled with TAMRA.

Antigen-Dependent Fluorescence of TAMRA-Labeled Anti-BGP scFv. The TAMRA-labeled anti-BGP scFv was purified using nickel-affinity chromatography and its fluorescence spectrum was measured in the absence and presence of a cognate antigen BGP-C7 peptide (NH₂-RRFYGPV-COOH). To our surprise, the fluorescence spectrum showed a remarkable dose-dependent increase (5.6-fold) in intensity upon addition of BGP-C7 (Figure 2A). A titration curve of the fluorescence intensity at 580 nm suggested that fluorescence increases with BGP-C7 peptide concentration (Figure 2B). Also, when the same measurement was performed with full-length BGP, similar dose-dependent fluorescence increase (max 5.2-fold) was observed. Using curve fitting, the ED₅₀ values for the peptide and the protein were estimated as 2.5×10^{-8} and 1.1×10^{-7} M, respectively, which compare well with the ED₅₀ value obtained by competitive ELISA (8.8×10^{-8} M for BGP-C7).⁹ The result indicates that the BGP peptide-binding activity of scFv had not been affected by the incorporation of TAMRA-C6-AF at the N-terminal region. To test if the observed fluorescence change could be used for imaging purposes, the fluorescence intensity of TAMRA-scFv was visualized in a 384-well microplate, in the presence and absence of the BGP peptide. The fluorogram obtained confirmed that the TAMRA-labeled scFv could potentially be used for quantitative imaging of the antigen in situ (Figure 2C).

To further evaluate the binding specificity of TAMRA-scFv, the same assay was performed with the somewhat longer peptides BGP-C10 (NH₂-EAYRRFYGPV-COOH, MW = 1257) and BGP-C10dV (NH₂-EAYRRFYGP-COOH, MW = 1158). The former includes the C-terminal valine that is an essential epitope of this antibody, while the latter lacks this residue.⁹ Titration curves indicated that while BGP-C10 showed a similar 5.8-fold increase to that observed for BGP-C7, no apparent

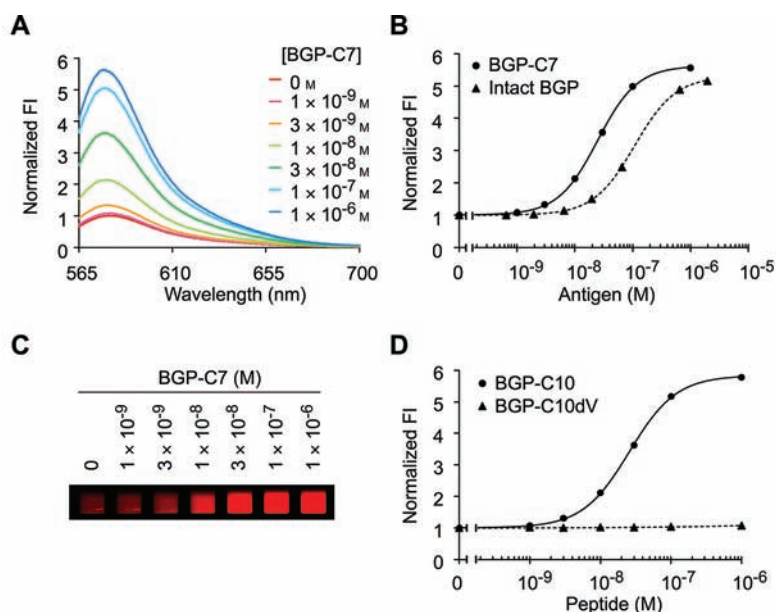


Figure 2. Antigen-dependent fluorescence enhancement of TAMRA-labeled anti-BGP scFv. (A) Fluorescence spectra of TAMRA-scFv with excitation at 550 nm in the absence and presence of BGP-C7 peptide. (B) Titration curve of the fluorescence intensity at 580 nm. The intensities are relative values with respect to that in the absence of BGP-C7 peptide. (C) Fluorescence imaging of TAMRA-scFv on a microplate in the presence of BGP-C7 peptide with excitation at 532 nm and emission at 580 nm. (D) Titration curves of TAMRA-scFv for BGP-C10 and BGP-C10dV peptides.

increase in fluorescence was observed in the presence of BGP-C10dV (Figure 2D). This clearly suggests that the binding specificity as well as the affinity of scFv for BGP is preserved, even in the presence of the N-terminal TAMRA dye.

Quenching of TAMRA Fluorescence by Trp Residues. Since the BGP peptides tested did not contain moieties capable of enhancing the TAMRA fluorescence, and no other dyes that might cause FRET between them were present either in the antigen or the antibody, we reasoned that the observed fluorescence enhancement mechanism involved electron transfer, rather than FRET. It has been reported previously that a number of organic fluorophores are quenched by Trp residues, either in solution or in a polypeptide. This quenching is thought to occur via a PET mechanism.^{12–14} We therefore investigated the possibility that the observed fluorescence intensity change was attributable to intramolecular quenching by Trp residues in scFv. The V_H fragment of this antibody has four Trp residues, namely, Trp33_H, Trp36_H, Trp47_H, and Trp103_H (using the Kabat numbering scheme¹⁵), while the V_L fragment has a single residue, Trp35_L. Almost all of these Trp residues, with the exception of Trp33_H, are located in the framework region, and are generally conserved in antibodies derived from various origins. A three-dimensional model (Figure 3A) suggested that Trp47_H and Trp103_H contribute to the hydrophobic interaction with V_L , and that Trp33_H contributes to the interaction with the BGP peptide. Trp36_H and Trp35_L are located close to the interacting surfaces of V_H and V_L , respectively.

To evaluate the potential role of the Trp residues on antigen-dependent fluorescence quenching, five Trp-to-Phe point mutants containing TAMRA-C6-AF were prepared, and the antigen-dependent fluorescence intensities were measured. All mutants showed significantly attenuated enhancements in fluorescence intensity upon addition of the BGP-C7 peptide, when compared to the wild-type scFv. Both the magnitude and the antigen-dependency

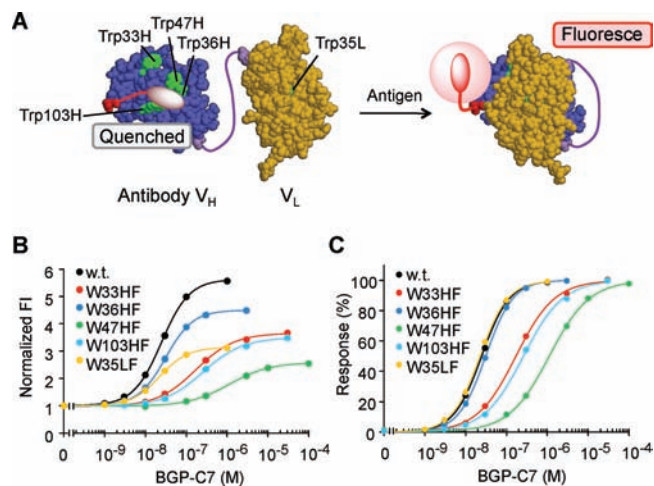


Figure 3. (A) The model of TAMRA-scFv. Structure for scFv was built using WAM antibody modeling server (<http://antibody.bath.ac.uk>) with CONGEN side chain building and Accessibility profile screen methods. Trp residues, Trp33_H, Trp36_H, Trp47_H, Trp103_H, and Trp35_L are colored green. (B) Titration curves of the Trp-to-Phe mutants. Fluorescence intensities are shown as relative values with respect to those in the absence of the antigen. (C) Normalized titration curves.

of fluorescence were diminished, depending on the mutation, although different behaviors were observed for different mutants (Figure 3B,C). Compared with the basal intensity without antigen, the fluorescence enhancements observed on addition of antigen were 3.7-, 4.7-, 2.5-, 3.5-, and 3.1-fold for the W33_HF, W36_HF, W47_HF, W103_HF, and W35_LF mutants, respectively. These values are all considerably less than the value observed for the wild-type scFv (5.6-fold). It is worth noting that a mutant of the Trp residue most distant to the TAMRA (W35_LF)

Table 1. Effect of Antigen and Denaturant (7 M GdnHCl, 100 mM DTT) on TAMRA Fluorescence

	λ_{\max}		normalized intensity at λ_{\max}		recovery ratio (%) ^a
	PBST + BGP-C7	PBST + denaturant	(A) + BGP-C7	(B) + denaturant	
5-TAMRA	573	580	1.0	1.1	-
w.t.	580	585	5.0	5.5	100
W33 _H F	580	585	3.8	4.2	100
W36 _H F	580	585	4.0	4.6	96
W47 _H F	580	585	2.2	2.6	93
W103 _H F	580	585	3.0	3.3	100
W35 _L F	580	585	2.4	3.0	88

^a Recovery ratio = $[A/(B/1.1)] \times 100$.

Table 2. Fluorescence Lifetimes τ_i , and Corresponding Amplitudes, a_i , of TAMRA Labeled Anti-BGP scFv in the Absence and Presence of 1 μ M BGP-C7 and Denaturant 7 M GdnHCl and 100 mM Dithiothreitol

	$\tau_1(\text{ns})/a_1$	$\tau_2(\text{ns})/a_2$
no BGP-C7	1.20/0.48	3.92/0.52
+ BGP-C7	1.46/0.21	3.75/0.79
Denaturant	3.14/1.00	

showed markedly reduced response, while fully maintaining its antigen dependency (i.e., binding affinity).

To further confirm the antigen-dependent removal of quenching mechanism proposed to explain the observed fluorescence enhancement, the fluorescence of TAMRA-scFv proteins under a denaturing condition was investigated. As summarized in Table 1, the fluorescence of free TAMRA and the proteins was measured in a standard buffer (PBS containing 0.05% Tween 20, PBST) or that containing 7 M guanidine hydrochloride (GdnHCl) and 100 mM dithiothreitol (DTT). While free TAMRA showed a modest (1.1-fold) fluorescence increase in the denaturant, the wild-type TAMRA-scFv showed a 5.5-fold increment, with a slight red shift in emission wavelength. The result is in accordance with our hypothesis that the quenching occurs in the folded protein, and this was removed by the denaturation, allowing the fluorescence to be revealed. On the other hand, the addition of BPG-C7 at saturating concentration to the wild-type TAMRA-scFv led to a 5.0-fold increment in fluorescence, supporting the “antigen-dependent release from the quenched state” hypothesis. The mutant TAMRA-scFv proteins showed diminished fluorescence increments upon denaturation, and also in the presence of saturated antigen. The observed increments were similar to each other (shown as recovery ratio in Table 1), indicating the active role of each Trp residue in the observed quenching. These results suggest that in the absence of antigen, the TAMRA fluorophore is in close proximity to these Trp residues. This includes the Trp35_L residue near the V_H/V_L interface, which may be able to interact with distant TAMRA due to the ProX tag sequence and the flexible aminohexyl linker between the scFv and the fluorophore. We postulate that the addition of antigen promotes the closure of the V_H/V_L interface, preventing the interaction of TAMRA with the Trp residues, and therefore removing the quenching.

Fluorescence Lifetime Measurement. To verify the occurrence of quenching and its release, fluorescence lifetime measurement of TAMRA-scFv was performed. Since multiple Trp

residues participate in quenching, the observed quenching was supposed to be dynamic rather than due to static interaction. In the case of dynamic quenching, faster fluorescence decay will be observed in the presence of quenchers.¹³ When fluorescence lifetime measurement was performed for TAMRA-scFv in the presence or absence of BGP-C7 peptide or denaturant, a significant difference in the amplitude of shorter lifetime species (1.2–1.46 ns) was observed (Table 2, Figure S1). In the presence of antigen or denaturant, longer lifetime species (3–4 ns, similar to reported values for free Trp^{16,17}) dominated. However, in the absence of these agents, the amplitude of shorter lifetime increased to almost half, clearly suggesting the occurrence of dynamic quenching probably due to a PET mechanism.

Fluorescence Correlation Spectroscopy Analysis. Depending on its concentration, scFv molecules can form dimers or other higher order species.¹⁸ Since TAMRA can form quenched dimer,¹⁹ there is a small possibility that the addition of antigen induced dissociation of a TAMRA-scFv oligomer to monomers, thus, resulted in increased species that emit brighter fluorescence. To rule out this possibility, fluorescence correlation spectroscopy (FCS) was utilized to measure the diffusion time of TAMRA-scFv, as a measure of its average molecular size in solution. As shown in Figure S2, compared with TAMRA-scFv alone, the addition of BGP-C7 or intact BGP resulted in increased diffusion time, which means slower diffusion probably due to increased molecular weight and possibly due to larger molecular size of scFv–antigen complex with exposed TAMRA dye. From this result and low scFv concentration used throughout this study, it is highly unlikely that the observed fluorescence increase was due to antigen-dependent increase of fluorescent monomers.

Effect of Dye Mobility. The observed fluorescence quenching may be resulted from the long, flexible linkage of the V_H N-terminus and the fluorophore. To confirm the effect of linker on quenching, flexible peptide linkers of (Gly₃Ser)_{*n*} (*n* = 1–3) were inserted between ProX tag and anti-BGP scFv to increase the mobility of the fluorophore (Figure 4A). Fluorescence spectral measurements showed that the antigen-dependent fluorescence increase was also observed for all the linker lengths while the response was slightly decreased for longer linkers (Figure 4B).

To evaluate the effect of the linker length further, an anti-bisphenol A scFv²⁰ was used as another recognition unit. The anti-bisphenol A scFv has six Trp residues including four conserved ones, which were expected to contribute to the fluorescence quenching as in the case of anti-BGP scFv (Table 3). The anti-bisphenol A scFv genes were constructed and expressed as TAMRA-labeled proteins in a similar manner. Fluorescence

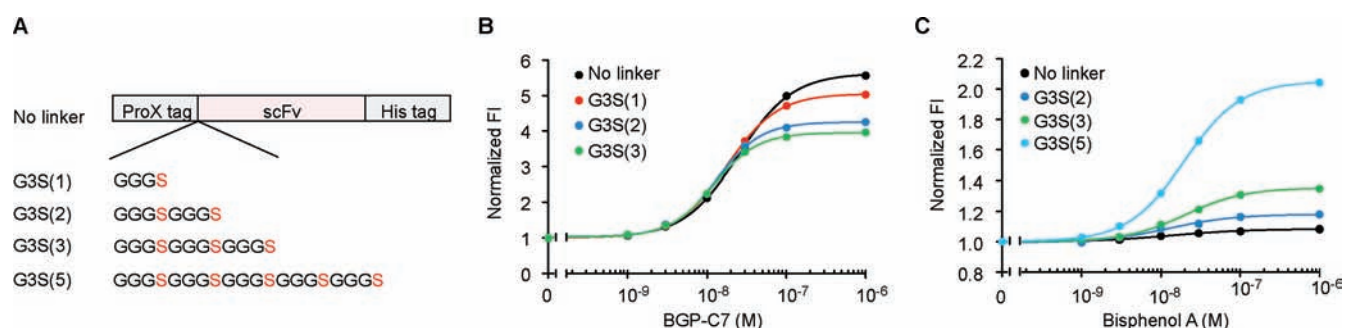


Figure 4. (A) Schematic structure of scFv containing flexible peptide linkers. (B) Titration curves of TAMRA-labeled anti-BGP scFVs with and without peptide linkers with excitation at 550 nm. Fluorescence intensities are relative values with respect to those in the absence of the antigen. (C) Titration curves of TAMRA-labeled anti-bisphenol A scFVs with and without peptide linkers with excitation at 550 nm. Fluorescence intensities are relative values with respect to those in the absence of the antigen.

Table 3. Locations of Trp Residues in the scFVs Used^a

	residue number																		
	CDRH1					CDRH3					CDRL3								
	H33	H34	H35	H36	...	H47	...	H95	...	H103	...	L35	...	L47	...	L91	L92	...	L94
α BGP	<u>W</u>	I	H	<u>W</u>		<u>W</u>		S		<u>W</u>		<u>W</u>		L		T	T		V
α Bisphenol A	Y	Y	<u>W</u>	<u>W</u>		<u>W</u>		V		<u>W</u>		<u>W</u>		I		S	<u>W</u>		I
α HEL	Y	<u>W</u>	S	<u>W</u>		Y		<u>W</u>		<u>W</u>		<u>W</u>		L		S	N		<u>W</u>
α BSA/HSA	A	M	A	<u>W</u>		<u>W</u>		S		<u>W</u>		<u>W</u>		L		A	D		S
α Estradiol	T	I	H	<u>W</u>		<u>W</u>		Y		<u>W</u>		<u>W</u>		<u>W</u>		<u>W</u>	S		Y
α Morphine	<u>W</u>	I	E	<u>W</u>		<u>W</u>		<u>W</u>		<u>W</u>		<u>W</u>		L		<u>W</u>	Y		N

^a Numbered according to Kabat.¹⁵

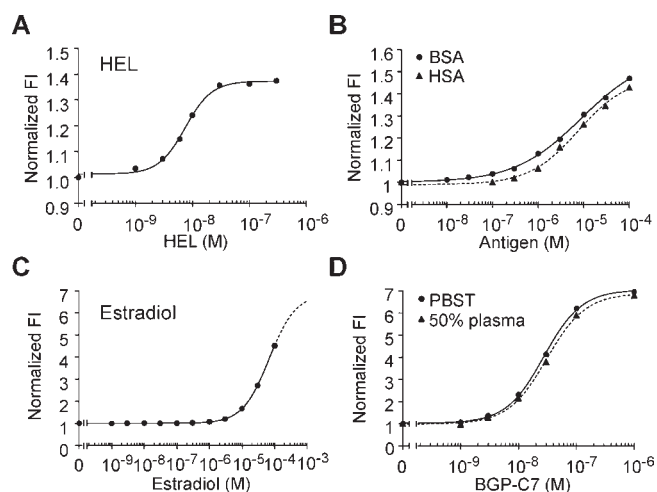


Figure 5. Titration curves of TAMRA-labeled scFVs. Fluorescence intensities are relative values with respect to those in the absence of the antigen. (A) HyHEL-10 for HEL, (B) 29Ij6 for BSA and HSA, (C) ES1-11 for estradiol. (D) Microplate-based imaging assay for BGP-C7 peptide either in 50% human plasma in PBST or in PBST buffer performed with TAMRA-labeled anti-BGP scFv. The TAMRA-scFv for A–C contain (Gly₃Ser)₂ linker, while that for D contains no linker.

spectra showed an increase in fluorescence intensity upon the addition of bisphenol A, although the observed response was much weaker (1.1-fold for the scFv without linker) than that of

the anti-BGP scFv (Figure 4C). Since this weak response may be due to suboptimal interaction between the fluorophore and Trp residues, elongation of the peptide linker was attempted. The insertion of (Gly₃Ser)_n linkers, in this case, markedly enhanced antigen-dependent fluorescence increase, and the scFv containing the longest (Gly₃Ser)₅ linker showed 2.0-fold fluorescence. From the fitting of titration curves, the EC₅₀ was estimated as 2.0 × 10⁻⁸ M, which was approaching to the IC₅₀ value determined by competitive ELISA for the original scFv (1.4 × 10⁻⁹ M).

Taken together, the results suggest that the insertion of peptide linker between the fluorophore and scFv affects the fluorescence quenching and its antigen-dependency. Although the exact reason of antibody-specific difference in response is unclear, this may be resulted from the difference in the optimal orientation of fluorophore to the differently positioned Trp residues in each scFv.

Application of the Quenchbody Strategy to Other scFVs.

We propose to name this position-specifically fluorolabeled scFv as a “quenchbody” after the quench phenomenon associated with it. Since many Trp residues are highly conserved in antibodies of various origins (see below), we expected that this approach might be broadly applicable to other antibody/antigen pairs. To further investigate this potential, we prepared quenchbodies for other antigens. First, hen egg lysozyme, 17 β -estradiol, and serum albumins (SAs) were used as model antigens. Examination of the primary sequence of these antibodies revealed that a number of Trp residues were conserved among them (Trp_{36H}, Trp_{47H}, Trp_{103H}, and Trp_{35L}) (Table 3). While anti-hen egg lysozyme

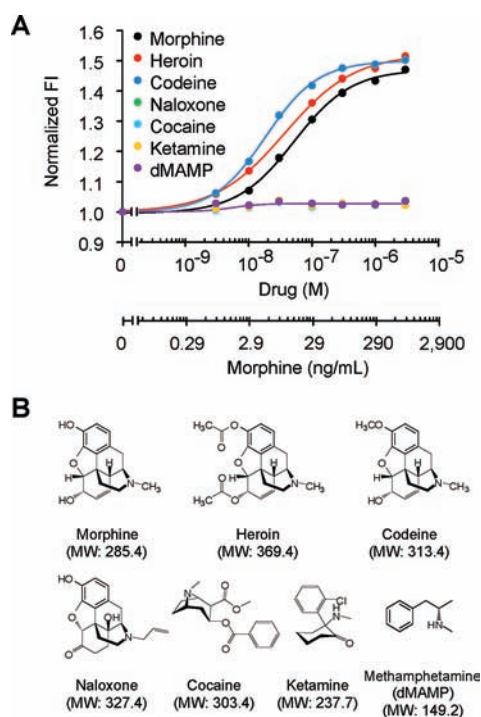


Figure 6. (A) Titration curves of TAMRA-labeled anti-morphine scFv for morphine and related drugs. Fluorescence intensities are relative values with respect to those in the absence of the antigen. (B) Molecular structure of the drugs with its molecular weight.

HyHEL-10 lacks Trp_{47H}, and anti-SA 29Ij6 contains only the conserved Trp residues, the number of Trp residues present in each scFv made us optimistic that antigen-dependent fluorescence would be observed.

To allow the performances of these antibodies to be compared under the same conditions, TAMRA-labeled quenchbodies containing the (Gly₃Ser)₂ linker between the ProX tag and the scFv were prepared as described above. The fluorescence intensity for the purified proteins in the absence and presence of their respective antigen were evaluated by fluorescence spectral measurements on titration with the antigens. As shown in Figure 5A–C, all the quenchbodies showed antigen-dependent fluorescence enhancements. However, the extent of enhancement was variable with the different scFvs. The anti-estradiol scFv showed the strongest antigen-dependent increase in fluorescence (4.5-fold increase), while the anti-lysozyme and anti-SA scFvs showed weaker responses (1.3- and 1.5-fold, respectively). However, it is worth noting that the calculated ED₅₀ for the lysozyme was 7.5×10^{-9} M, which is comparable to the reported K_d values of the Fv and scFv (5.0×10^{-9} and 1.2×10^{-8} M, respectively).²¹ The ED₅₀ measured for human SA ($\sim 10^{-5}$ M) was sufficiently lower than its reference range of 3.4–5.4 g/dL (0.5–0.8 mM) in serum (MedlinePlus, <http://www.nlm.nih.gov/medlineplus/ency/article/003480.htm>) to indicate its potential utility as a diagnostic reagent.

Measurement of BGP Peptide in Human Plasma. To further demonstrate the utility of quenchbodies in clinical diagnostic applications, the performance of the quenchbody in a plasma sample was investigated using a fluorescence imager. As shown in Figure 5D, the TAMRA-quenchbody for BGP showed an almost indistinguishable dose–response for the BGP-C7 peptide in

50% human plasma to that in PBST. The maximum fluorescence was as high as 7-fold of that observed in the absence of antigen. This result compares well with our previous open sandwich enzyme-linked immunosorbent assay (OS-ELISA) for BGP, which showed considerable signal reduction in serum-derived samples without pretreatment to remove SAs.²²

Application to Morphine Detection. Sensitive detection, identification, and confirmation of opiates are considered highly important in view of public health and crime prevention. However, most conventional analytical methods for opiates such as morphine or heroin are laborious and time-consuming. As another practical application of quenchbody technology, rapid detection of opiates was attempted. On the basis of the published nucleotide sequence of an scFv (V_L-V_H) recognizing morphine-6-glucuronide (M6G),²³ a quenchbody for M6G was prepared and investigated for its fluorescence spectra upon addition of morphine and related drugs (Figure 6B and Figure S3).

As shown in the dose–response curves in Figure 6A, the constructed quenchbody reacted most strongly with codeine, and also heroin and morphine in this order with the calculated EC₅₀ values of 1.9, 3.7, and 5.2×10^{-8} M, respectively. Although the maximum fluorescence increase was about 1.5-fold over the background, 1–100 ng/mL of these compounds were detectable within 3 min after reaction start. On the other hand, naloxone wherein the *N*-methyl group observed in opiates is substituted with *N*-propenyl, as well as cocaine, ketamine, and methamphetamine, showed negligible fluorescence increase, probably due to the absence of this *N*-methyl as the essential epitope.

To compare the antigen dose-dependency of quenchbody fluorescence with that of antigen binding, we performed competitive ELISA using immobilized morphine-BSA and free morphine, and the amount of bound quenchbody was evaluated using peroxidase-conjugated anti-His₅ antibody. From the curve-fitting, the IC₅₀ for morphine was obtained as 26 ± 12 nM (Figure S4), which was a similar value to the EC₅₀ of quenchbody fluorescence. These data suggest that the anti-morphine quenchbody could detect as little as parts per billion (ppb) range of opiates by just mixing the sample and measuring its fluorescence, which obviates the needs of long and dangerous reaction/washing steps inevitable in ELISA.

DISCUSSION

Our working model of the antigen-dependent quenchbody fluorescence observed with this system is as follows. In the absence of antigen, TAMRA within the ProX tag sequence penetrates between the V_H/V_L interface, and interacts with Trp residues by hydrophobic and/or π – π stacking interactions (Figure 3A). This interaction leads to a quenching electron transfer from the Trp residues to the dye due to transient contact between each Trp residue and the chromophore.^{13,14} Binding of an antigen, such as the BGP peptide, to the scFv induces tighter complexation of V_H and V_L, and thus releases the TAMRA dye from interactions with the Trp residues near the V_H/V_L interface.

Among the five tryptophans found to be responsible for the quenching of the TAMRA-labeled anti-BGP quenchbody, four (Trp_{36H}, Trp_{47H}, Trp_{103H}, and Trp_{35L}) are located in the framework region, and are highly conserved among immunoglobulins of various origins. According to a database of >35 000 nonredundant immunoglobulin sequences (Abysis, <http://bioinf.org.uk/>), the rate of conservation for the three H chain tryptophans is 99.0%, 93.3%, and 97.0%, respectively, and that for

Trp 35_L is 98.0%, for 12 483 chains including kappa and lambda chains. These values, as well as the number of Trp residues involved, ensure that almost all Fv could potentially be successfully incorporated into a quenchbody. It is interesting that while the side chain of Trp35_L is located in the protein core, and therefore is not exposed to solvent in any antibody structure, it plays a considerable role in the quenching effect observed in the anti-BGP quenchbody. Presumably, the dynamics of the scFv's polypeptide backbone might result in transient escape of this residue from the buried hydrophobic core, and/or penetration of hydrophobic TAMRA dye into the vicinity of this residue.

In the anti-BGP quenchbody, additional quenching by Trp33_H was observed. This CDR2 residue is likely to be in the antigen-binding site, and therefore, the presence of TAMRA in close proximity to this residue would be prohibited by antigen binding, which therefore inhibits quenching and enhances fluorescence. It can be speculated that the different fluorescence dynamic ranges observed for the quenchbodies based on different antibodies is due to differences in their Trp residue content, both in number and in positions. As shown in Table 3, some scFvs contain Trp residues in addition to the conserved ones. For example, anti-estradiol scFv, whose quenchbody showed a large fluorescence increase, has two additional Trp residues in V_L. These may contribute to enhancing the quenching effect. On the other hand, the anti-SA scFv obtained from a synthetic phage library, Tomlinson J,²⁴ has no Trp other than the conserved ones, and its quenchbody demonstrated a lower response. Nonetheless, the obtained results overall suggest that the conserved Trp residues are sufficient per se for an antigen-dependent fluorescence quenching effect to be observed. Therefore, the present strategy can be expected to be effective for various scFvs, including those with minimal conserved Trp residues. An improved response is likely for those scFvs containing additional residues, depending on their number and positions.

The putative working mechanism also suggests that antibodies that show a higher antigen-dependent stabilization (larger signal change in OS-ELISA that detects the interaction between V_H and V_L)²⁵ are likely to show more fluorescence activation. This is because these antibodies have a higher chance of having a solvent-exposed V_H/V_L interface. However, while fluorescence activation was observed for the anti-SA scFv, the same Fv showed a minimal response to BSA in a phage-based OS-ELISA.²⁶ It is likely that a small antigen-dependent change in V_H/V_L interaction strength is sufficient to obtain an observable change in fluorescence intensity. This implies that quenchbodies can be applied not only to small molecule detection, but also to the detection of various protein antigens, even if they contain several Trp residues.

PET is recognized as a useful mechanism to alter the fluorescence of organic dyes and their derivatives using small molecules such as metal ions or reactive oxygen species.^{27,28} Only recently, it has been found to be useful in the detection of natural biomolecules such as guanine²⁹ and tryptophan.¹³ Several organic fluorochromes have been shown quenched by tryptophans, either by an intermolecular or intramolecular PET mechanism. For example, ATTO 655-labeled streptavidin was efficiently quenched probably due to the spatial proximity of the fluorolabeled Lys residues to Trp residues in streptavidin. The observed quenching effect was markedly reduced in the presence of streptavidin's ligand biotin.¹³ When compared with this system, the quenchbody system has the benefit of a large range of detectable targets.

CONCLUSION

We reported a discovery of novel biosensing principle utilizing fluorescence quenching of a labeled dye by intrinsic Trp residues in antibody Fv region. Compared with conventional fluoro-immunoassays, the quenchbody assay is simple, and requires no additional reagents to perform the detection. In addition, compared with OS-ELISA using Fv molecules, scFv-based quenchbodies generally show higher sensitivity due to the linkage of the two variable region fragments. Another merit of this scFv-based system is their ready availability, as specific scFvs can be directly obtained from phage-display libraries of various origins. Because of the simplicity of the system, the application of quenchbodies is not likely to be limited to in vitro diagnostics, but may also be applied to imaging in situ or in vivo. In future, the development of more robust quenchbody production methods, such as in vivo incorporation of non-natural amino acids,³⁰ will further enlarge the scope of their applications.

EXPERIMENTAL METHODS

Materials. In-Fusion Advantage PCR Cloning Kit was from Takara Bio (Otsu, Japan). A pIVEX2.3d vector and RTS 100 *E. coli* Disulfide Kit were from Roche Diagnostics (Basel, Switzerland) or 5-Prime GmbH (Hamburg, Germany). C-terminal peptides for human osteocalcin (bone gla protein, BGP) (BGP-C7, NH₂-RRFYGPV-COOH, MW = 894; BGP-C10, NH₂-EAYRRFYGPV-COOH, MW = 1257; BGP-C10dV, NH₂-EAYRRFYGP-COOH, MW = 1158) were obtained from GenScript (Piscaway, NJ). Bovine serum albumin (BSA) was from Bovogen (Essendon, Australia). Hen egg lysozyme (HEL) was from Wako (Tokyo, Japan). Human serum albumin (HSA) and 17 β -estradiol were from Sigma (Saint Louis, MO). Pooled normal human plasma was from Innovative Research (Northville, MI).

Construction of scFv Genes. An expression vector, pROX-BGP-scFv, harboring a T7 promoter-controlled scFv gene of anti-BGP C-terminal fragment KTM-219⁹ fused with an N-terminal ProX tag containing an amber codon (ATG TCT AAA CAA ATC GAA GTA AAC TAG TCT AAT GAG) and a C-terminal His tag was constructed by overlap PCR. A 15-amino acid linker with three Gly₄-Ser repeats was inserted between the V_H and V_L. The V_H chain was amplified using the 5'-primer (CTTTAAGAAGGAGATATACCATGTCTAAACAAATC-GAAGTAAACTAGTCTAATGAGACCCAAAGTAAAGCTGCAGCAGT-C) and the 3'-primer (CCAGAGCCACCTCCGCCTGAACCGCCTCCACCGCTCGAGACGGTGC), and the V_L chain was amplified using the 5'-primer (CAGGCGGAGGTGGCTCTGGCGGTGGCGGATCTGACATTGAGCTCACCC) and the 3'-primer (TGATGATGAGAACCCCCCCCCGTTTTATTTCAG). The amplified V_H and V_L genes were linked by overlap PCR using the V_H 3'-primer and the V_L 5'-primer, and the construct was then cloned into *Nco*I- and *Sma*I-digested pIVEX2.3d using an In-Fusion PCR cloning kit.

A wild-type (nonlabeled) scFv was constructed by replacing the TAG codon with a TTT codon in the ProX tag. For substitution of tryptophan (Trp) residues with phenylalanine (Phe), TGG codons for Trp33, Trp36, Trp47, and Trp103 in the V_H gene, and Trp35 in the V_L gene were each replaced by a TTT codon. For scFv genes encoding anti-BGP and anti-bisphenol A,²⁰ the corresponding genes were cloned in place of anti-BGP scFv, with an additional sequence encoding N-terminal (G₃S)₀₋₅ linker. For scFv genes encoding anti-hen egg lysozyme,³¹ bovine serum albumin (BSA),²⁶ and estradiol (Fujioka et al., in preparation), the corresponding genes were cloned in place of anti-BGP scFv, with an additional sequence encoding N-terminal (G₃S)₂ linker. The anti-morphine-3-glucuronide scFv gene was synthesized by Mr. Gene GmbH (Regensburg, Germany) according to the published sequence for clone E3,²⁵ assuming that the undisclosed heavy chain FR4

sequence was derived of J4 segment. The gene for V_L-V_H type scFv with N-terminal (G₃S)₂ and internal (G₄S)₄ linkers was inserted to pROX-BGP-scFv in place of anti-BGP scFv as above.

Preparation of Aminoacyl tRNA. TAMRA-C6-AF-pdCpA was synthesized as described previously.¹⁰ This was ligated to an amber suppressor tRNA, derived from *M. capricolum* Trp₁ tRNA without the 3' dinucleotide, by chemical ligation as described previously.^{11,32} The aminoacyl-tRNAs can be obtained as commercially available reagents (CoverDirect tRNA reagents for site-directed protein labeling, Protein Express, Chiba, Japan).

Cell-free Transcription/Translation. The incorporation of TAMRA-C6-AF into the N-terminal region of scFv was performed using an RTS 100 *E. coli* Disulfide kit. The reaction mixture (50 μ L) comprised 7 μ L of an amino acid mix, 1 μ L of methionine, 7 μ L of the reaction mixture, 25 μ L of activated *E. coli* lysate, 5 μ L of plasmid DNA (500 ng), and 5 μ L of TAMRA-C6-AF-tRNA (0.8 nmol). All the reagents used, with the exception of the plasmid and the tRNA, were provided in the RTS 100 *E. coli* Disulfide kit. The reaction mixture was incubated at 20 °C with shaking on RTS ProteoMaster (Roche Diagnostics, Basel, Switzerland) at 600 rpm for 2 h, and subsequently at 4 °C without shaking for 16 h. An aliquot of the reaction mixture (0.5 μ L) was applied to 15% SDS-PAGE³³ and the gel was visualized using a fluorescence scanner FMBIO-III (Hitachi, Tokyo, Japan). The gel was also analyzed by Western blot analysis using anti-His tag (Novagen, La Jolla, CA) and alkaline phosphatase-labeled anti-mouse IgG (Promega, Madison, WI).

To purify scFv, the reaction mixture (50 μ L) was diluted in wash buffer (20 mM phosphate, 0.5 M NaCl, 60 mM imidazole, 0.1% polyoxyethylene(23)lauryl ether, pH 7.4) to a final volume of 400 μ L, and applied to a His Spin Trap Column (GE Healthcare, Piscataway, NJ). After incubation at room temperature for 15 min, the column was washed three times with wash buffer. The labeled scFv proteins were eluted with two 200 μ L volumes of wash buffer containing 0.5 M imidazole. The eluate was passed through an UltraFree-0.5 centrifugal device (Millipore, Billerica, MA) and equilibrated with phosphate buffered saline Tween-20 (PBST, 10 mM phosphate, 137 mM NaCl, 2.7 mM KCl, 0.05% Tween-20, pH 7.4) to allow buffer exchange and concentration of the protein. The concentration of the labeled scFv protein was determined by comparing the fluorescence intensities of a known concentration of TAMRA dye (Anaspec, Fremont, CA) and the sample under denaturing conditions in 7 M guanidine hydrochloride, pH 7.4.

Fluorescence Measurements of TAMRA-labeled scFvs. For fluorescence spectral measurements of anti-BGP scFv, the purified scFv (2 μ g/mL, 25 μ L) was diluted in 200 μ L of PBST containing 0.2% BSA, and BGP peptide was added by titration in a 3 \times 3 mm quartz cell (GL Sciences, Tokyo, Japan). After each addition of the antigen, the solution was incubated at 25 °C, 70 min prior to the fluorescence spectral measurements.

Anti-lysozyme HyHEL-10, anti-estradiol, and anti-M3G scFvs (2 μ g/mL, 25 μ L) were diluted in PBST containing 1% BSA. Anti-SA scFv 29IJ6 (2 μ g/mL, 25 μ L) was diluted in PBST containing 0.2% gelatin. The antigens were added by titration at 5 min intervals, except for anti-M3G, to which antigens were added at 3 min intervals.

Fluorescence spectra were measured from 565 to 700 nm, with excitation at 550 nm at 25 °C on a FluoroMax-4 (Horiba Jobin-Yvon, Kyoto, Japan). Excitation and emission slit widths were set to 5.0 nm. The ED₅₀ values were calculated by curve fitting of the observed fluorescence intensities at the maximum emission wavelength, using a sigmoidal dose-response model based on ImageJ software (<http://rsbweb.nih.gov/ij/>).

For fluorescence imaging of anti-BGP scFv, the purified scFv (2 μ g/mL, 6.25 μ L) was mixed with various concentrations of the antigen in PBST (50 μ L) containing BSA (0.2%), or in 50% human plasma from which the endogenous antigen had been removed,²² in a 384-well microplate (Olympus, Tokyo, Japan). The plate was visualized with excitation at 532 nm and emission at 580 nm using a fluorescence scanner.

Fluorescence lifetime measurements were performed on a TemPro system (Horiba Jobin-Yvon, Japan) using the time-correlated single-photon counting (TCSPC) technique. The excitation source was a 495 nm SpectraLED with a pulse length of \sim 1 ns at a repetition rate of 1 MHz. Emission at $>$ 600 nm was collected using a long-pass filter SCF-50S-60R (SIGMA KOKI), and the decay parameters were determined by least-squares deconvolution.

Abbreviations. BGP, bone gla protein (osteocalcin); BPA, bisphenol A; CDR, complementarity determining region; dNTPs, deoxyribonucleotide triphosphate; ELISA, enzyme-linked immunosorbent assay; FCS, fluorescence correlation spectroscopy; Fv, antibody variable region fragments; PBS, phosphate buffered saline; PBST, PBS containing 0.05% Tween 20; PCR, polymerase chain reaction; scFv, single chain antibody variable region fragment.

■ ASSOCIATED CONTENT

S Supporting Information. Decay curves obtained in the fluorescence lifetime measurements, FCS data and methods, fluorescence spectra for TAMRA-scFv specific to M3G, and competition ELISA result for morphine. This material is available free of charge via the Internet at <http://pubs.acs.org>.

■ AUTHOR INFORMATION

Corresponding Author

hueda@chembio.t.u-tokyo.ac.jp

Present Addresses

^{||}Department of Bioscience and Biotechnology, Faculty of Agriculture, Shinshu University, Nagano, Japan.

■ ACKNOWLEDGMENT

We are indebted to T. Ueda, Y. Ohya, N. Tomioka, T. Saganuma, and S. Ebisu for valuable suggestions, T. Shinoda for anti-BGP gene, H. Ohkawa for anti-BPA gene, I. Tomlinson for anti-SA gene, and Y. Fujioka for anti-E2 gene. We also thank Y. Mizuta, N. Teshigawara and M. Nakamura in Central Customs Lab., Ministry of Finance, Japan, for their help in morphine measurement. This project was partly supported by City-area program from MEXT, Japan, a Grant-in-Aid for Scientific Research (B20360368) from JSPS, Japan, a Grant-in-Aid for Scientific Research on Innovative Areas (20107005) from MEXT, Japan, and by the Global COE Program for Chemistry Innovation, MEXT, Japan.

■ REFERENCES

- (1) Jones, G.; Lu, L. N.; Vullev, V.; Gosztola, D. J.; Greenfield, S. R.; Wasielewski, M. R. *Bioorg. Med. Chem. Lett.* **1995**, *5*, 2385–2390.
- (2) Neuweiler, H.; Schulz, A.; Vaiana, A. C.; Smith, J. C.; Kaul, S.; Wolfrum, J.; Sauer, M. *Angew. Chem., Int. Ed.* **2002**, *41*, 4769–4773.
- (3) Knemeyer, J. P.; Marme, N.; Sauer, M. *Anal. Chem.* **2000**, *72*, 3717–3724.
- (4) North, J. R. *Trends Biotechnol.* **1985**, *3*, 180–186.
- (5) Pollack, S. J.; Nakayama, G. R.; Schultz, P. G. *Science* **1988**, *242*, 1038–1040.
- (6) Renard, M.; Belkad, L.; Hugo, N.; England, P.; Altschuh, D. I.; Bedouelle, H. *J. Mol. Biol.* **2002**, *318*, 429–442.
- (7) Jespers, L.; P. Bonnert, T.; Winter, G. *Protein Eng., Des. Sel.* **2004**, *17*, 709–713.
- (8) Hohsaka, T.; Kajihara, D.; Ashizuka, Y.; Murakami, H.; Sisido, M. *J. Am. Chem. Soc.* **1999**, *121*, 34–40.

- (9) Lim, S.-L.; Ichinose, H.; Shinoda, T.; Ueda, H. *Anal. Chem.* **2007**, *79*, 6193–6200.
- (10) Abe, R.; Shiraga, K.; Ebisu, S.; Takagi, H.; Hohsaka, T. *J. Biosci. Bioeng.* **2010**, *110*, 32–38.
- (11) Taira, H.; Matsushita, Y.; Kojima, K.; Shiraga, K.; Hohsaka, T. *Biochem. Biophys. Res. Commun.* **2008**, *374*, 304–308.
- (12) Buschmann, V.; Weston, K. D.; Sauer, M. *Bioconjugate Chem.* **2003**, *14*, 195–204.
- (13) Marmé, N.; Knemeyer, J.-P.; Sauer, M.; Wolfrum, J. *Bioconjugate Chem.* **2003**, *14*, 1133–1139.
- (14) Vaiana, A. C.; Neuweiler, H.; Schulz, A.; Wolfrum, J.; Sauer, M.; Smith, J. C. *J. Am. Chem. Soc.* **2003**, *125*, 14564–14572.
- (15) Kabat, E. A.; Wu, T. T.; Perry, H. M.; Gottesman, K. S.; Foeller, C. *Sequences of Proteins of Immunological Interest*, 5th ed.; U.S. Government Printing Office: Bethesda, MD, 1991.
- (16) Edman, L.; Mets, Ü.; Rigler, R. *Proc. Natl. Acad. Sci. U.S.A.* **1996**, *93*, 6710–6715.
- (17) Wennmalm, S.; Edman, L.; Rigler, R. *Proc. Natl. Acad. Sci. U.S.A.* **1997**, *94*, 10641–10646.
- (18) Raag, R.; Whitlow, M. *FASEB J.* **1995**, *9*, 73–80.
- (19) Ogawa, M.; Kosaka, N.; Choyke, P. L.; Kobayashi, H. *ACS Chem. Biol.* **2009**, *4*, 535–546.
- (20) Nishi, K.; Takai, M.; Morimune, K.; Ohkawa, H. *Biosci., Biotechnol., Biochem.* **2003**, *67*, 1358–1367.
- (21) Tsumoto, K.; Nakaoki, Y.; Ueda, Y.; Ogasahara, K.; Yutani, K.; Watanabe, K.; Kumagai, I. *Biochem. Biophys. Res. Commun.* **1994**, *201*, 546–551.
- (22) Ihara, M.; Yoshikawa, A.; Wu, Y.; Takahashi, H.; Mawatari, K.; Shimura, K.; Sato, K.; Kitamori, T.; Ueda, H. *Lab Chip* **2010**, *10*, 92–100.
- (23) Dillon, P. P.; Manning, B. M.; Daly, S. J.; Killard, A. J.; O’Kennedy, R. *J. Immunol. Methods* **2003**, *276*, 151–161.
- (24) de Wildt, R. M.; Mundy, C. R.; Gorick, B. D.; Tomlinson, I. M. *Nat. Biotechnol.* **2000**, *18*, 989–994.
- (25) Ueda, H.; Tsumoto, K.; Kubota, K.; Suzuki, E.; Nagamune, T.; Nishimura, H.; Schueler, P. A.; Winter, G.; Kumagai, I.; Mahoney, W. C. *Nat. Biotechnol.* **1996**, *14*, 1714–1718.
- (26) Aburatani, T.; Ueda, H.; Nagamune, T. *J. Biochem.* **2002**, *132*, 775–782.
- (27) Silva, A. P. d.; Fox, D. B.; Moody, T. S.; M. Weir, S. *Trends Biotechnol.* **2001**, *19*, 29–34.
- (28) Koide, Y.; Urano, Y.; Kenmoku, S.; Kojima, H.; Nagano, T. *J. Am. Chem. Soc.* **2007**, *129*, 10324–10325.
- (29) Torimura, M.; Kurata, S.; Yamada, K.; Yokomaku, T.; Kamagata, Y.; Kanagawa, T.; Kurane, R. *Anal. Sci.* **2001**, *17*, 155–160.
- (30) Sakamoto, K.; Murayama, K.; Oki, K.; Iraha, F.; Kato-Murayama, M.; Takahashi, M.; Ohtake, K.; Kobayashi, T.; Kuramitsu, S.; Shirouzu, M.; Yokoyama, S. *Structure* **2009**, *17*, 335–344.
- (31) Neri, D.; Momo, M.; Prospero, T.; Winter, G. *J. Mol. Biol.* **1995**, *246*, 367–373.
- (32) Iijima, I.; Hohsaka, T. *ChemBioChem* **2009**, *10*, 999–1006.
- (33) Laemmli, U. K. *Nature* **1970**, *227*, 680–685.